NRIAG JOURNAL OF ASTRONOMY AND GEOPHYSICS
2023, VOL. 12, NO. 1, 45–57
https://doi.org/10.1080/20909977.2022.2163787

2D electrical resistivity tomography (ERT) investigation of a landslide: A case study from Ali Mendjeli, Constantine, North-East of Algeria

Ammar Chibani[a], Kamel Hebbache[b], Mekki Mellas[a] and Abdelhak Mabrouki[a]

[a]Civil Engineering Research Laboratory (LRGC), Department of Civil Engineering and Hydraulics, University of Mohamed Khider, BP 145, 07000, Biskra, Algeria; [b]Department of Civil Engineering, University of Ferhat Abbas, Setif, Algeria

ABSTRACT

Constantine is city characterised by a very rugged relief in which frequently happened the collapse of buildings as a result of landslide hazards. The aims of this study are to determine the depth of the surface landslide and to evaluate the landslide mass in the new city of Ali Mendjeli, which is nearby Constantine in Northeastern Algeria, using a geophysical method, namely the electrical resistivity tomography (ERT). Five two-dimensional (2D) ERT profiles were performed along and across the landslide using Wenner electrode array. Two parallel profiles to the sliding direction of 69 m length of each profile and three other perpendicular profiles, each with a length of 115 m, were conducted with inter-electrode spacing of 3 and 5 m, respectively. The resistivity data processing was carried out using *Res2Dinv* software. The inverted pseudo-section models presented formations characterised by low resistivities which can be summarised in two sets ranging from 1.38 to 6.20 Ωm and from 6.20 to 19 Ωm. The inverted resistivity data were correlated and calibrated with respect to the subsoil lithology obtained by well drilling and inclinometer tests. According to the inclinometer displacements, the measurements were of the order of 2–3 mm for a depth of 10 m and between 17.5 and 19.5 m for a depth of 13 m. The combined measurements of ERT and the geotechnical testing not only have shown a good agreement in the results obtained but also have successfully detected the depth of probable rupture surfaces and displaced materials likely to slip. This concordance of the obtained results. The estimated volume of the sliding material was around 20.000 m^3. According to the obtained results of this study, ERT can be applied to detect sliding surfaces in landslides.

ARTICLE HISTORY
Received 25 September 2022
Revised 14 December 2022
Accepted 26 December 2022

KEYWORDS
Electrical resistivity tomography; landslide; wenner array; geotechnical investigations; surface rupture

1. Introduction

Landslides are among the catastrophic and the most existing natural risks that affect larger regions worldwide and cause significant damages in terms of both mankind lives and material. These threats affect basic infrastructures and urban development (structures, roads, highways, dams, etc.) and disrupt various networks. They require in-depth inspections due to their structural complexities and topographic extents. Hard work conditions make recognition's interventions difficult and costly (Kherrouba et al. 2018). Remote sensing and geophysical methods including Image Acquisition Systems, Geosensors, Terrestrial Laser Scanner (TLS), Seismic Surveys (SS), ERT (ERT) and other recent methods (Margottini et al. 2013; Casagli et al. 2020; Jongmans et al. 2020) offer the possibility to investigate these kinds of hazards and to predict the failure time and risk management, either to clearly defining the landslide structure and the sliding surface depth. Among of these techniques, ERT (Hebbache and Boubaya Djajo 2022), is a promising geophysical tool frequently applied to obtain high resolution subsurface resistivity distribution models (mHebbache et al. 2016; Cubbage et al. 2017; Nordiana et al. 2018; Osinowo and Falufosi 2018). Owing to ERT effectiveness in landslide applications, several case studies have been reported worldwide (Bogoslovsky and Ogilvy 1977; Crawford et al. 2015; Falae et al. 2019; Zhuang and Xing 2020; Tunçel et al. 2021) to evaluate the failure investigation slope and to delimit the landslide geometry (Giano et al. 2000; Ismail and Yaacob 2018; Rezaei et al. 2018). ERT is used in landslide investigations owing to its high sensitivity to water saturation in bedrock and colluvium, a critical factor generating landslides. Akpan et al. (2015) have evaluated the internal landslide area structure and have deduced the role of groundwater flow in the landslide activity starting point based on both geophysical techniques of the electrical resistivity and seismic refractions. Ismail and Yaacob (2018) through the use of the 2D resistivity have identified the ERT behaviour beneath a slope area by predicting the failure surface position. They have reported that the use of ERT in conjunction with borehole's drillings are useful tools for characterising slope failures through subsurface profiles and the subsoil properties. Cubbage et al. (2017) have investigated the internal structure, the sliding surface and the discontinuities in an unstable landslide part of Ain Torki

CONTACT Kamel Hebbache hebbache.kamel@univ-setif.dz Department of Civil Engineering, University of Ferhat Abbas, Bejaia Road Setif, 19000 Algeria

(North of Algeria) based on ERT. They have concluded that the sliding surface is the limit between the relatively high resistivity mobile material and the underlying conductive marls. This agrees with the lithological data from boreholes, which show a depth to unweathered marls of about 10–15 m. Rezaei et al. (2018) have used ERT along boreholes data to investigate the relationship between geotechnical and geophysical parameters within Nargeschal landslide area, a good correlation was reported. Samodra et al. (2020) have analysed the data recorded of a landslide using multi-temporal UAV and ERT techniques. These were used for detecting and characterising the displacement and internal structure of the landslide. They analysed the different factors that affect internal structure displacements. The combination of geophysical and geotechnical investigations leads to a better understanding of landslides and subsoil movement formations (Lee et al. 2008; Reci et al. 2013).

In Algeria, landslides are a serious problem that requires immediate care and attention from the authorities. The prime aim of this study is to use 2D electrical resistivity method combined with geotechnical tests in order to investigate the internal structure and the sliding surface of a particular area located in the northeastern region of Algeria (Figure 1).

2. General geography

Geographically the investigated area falls within latitudes 36°13′33.24″N and 36°13′39.15″N and longitudes 6°31′52.59″E and 6°31′56.11″E, at a mean elevation of ~726 m above sea level (a.s.l.). The studied site is located in the vicinity of the wilaya road no. 101, which connects the new city of Ali Mendjeli and Ain Smara in the southwest suburbs of Constantine (NE of Algeria).

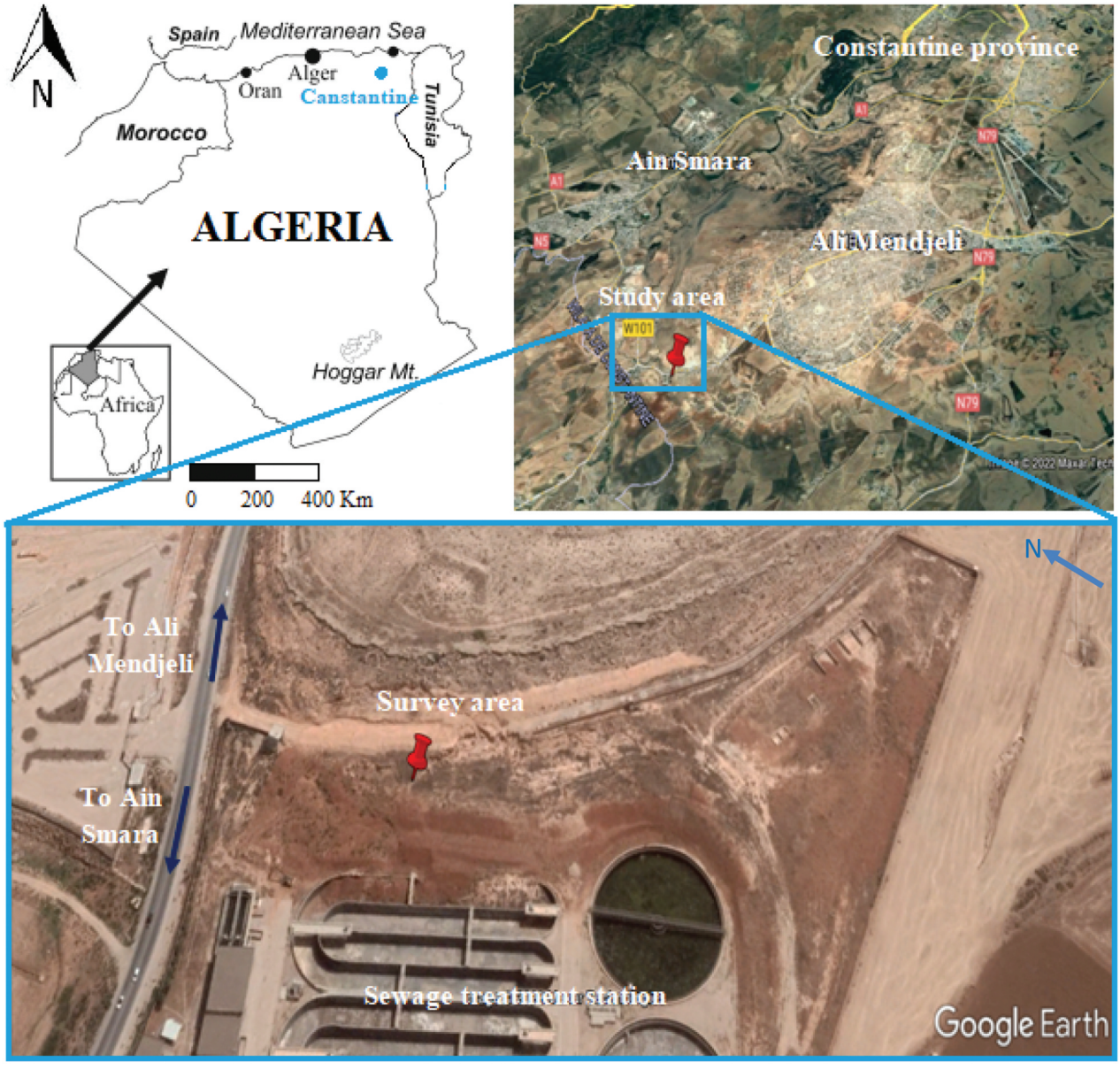

Figure 1. Satellite photo showing the study area.

3. Geological and hydrogeological background

Constantine belongs to the neogene basin post-nappes of Constantine. This basin is oriented ENE-WSW and is located in the Atlas tellian of alpine chain. The geological formations present in the Constantine basin include the substratum formations which are essentially constituted by massive limestone of the upper cretaceous (Cenomano-turonian), marls and marly of the cretaceous (Tellian) and the post-napped formations (Coiffait 1992). The Miocene is represented by several facies of thick breccia at the base then red clays, conglomerates, gypsum marls and sandstones. The Pliocene is only known in the southern part of the basin. Discordant on the Miocene formations, it is represented by black clays at the base and lacustrine limestone. The Quaternary is represented by lacustrine limestone sometimes travertine with their sandy-conglomerate base and the alluvial terraces of the river Rhumel and Boumerzoug. The other formations correspond to heterogeneous slope deposits, not very thick. The site of our study interest belongs to the sedimentary formations on an outcrop of Pliocene-Villafranchian: continental lacustrine deposits, limestone and lacustrine marls (tuffaceous), breccias, conglomerates, coarse sandstones, sandstones and continental sands (Figure 2) (referenced sheet N°: 96B6–C26). Facies of the main fillings of the basins are hard or cavernous travertine limestone, red, pinkish or brownish, often of very vivid hue and reddish or pinkish marls continuation of the lacustrine limestone of Hadj-Baba and Ain El-Bey. Coastal facies lacustrine: banks of red conglomerates more or less consolidated, alternating with red marls and red breccias passing laterally to the preceding deposits that of the geological side (Coiffait 1992). From a hydrogeological point of view, the site is located in the south-west of the new city Ali Mendjeli. It belongs to the watershed hydrographic basin of Kebir-Rhumel and its sub-basin Rhumel-Seguin. This exoreic basin is characterised by a great hydrogeological complexity. It is drained by two important rivers. In the southern part, Oued Rhumel, and in the western part, Oued Enndja. Their confluence downstream gives Oued Kebir

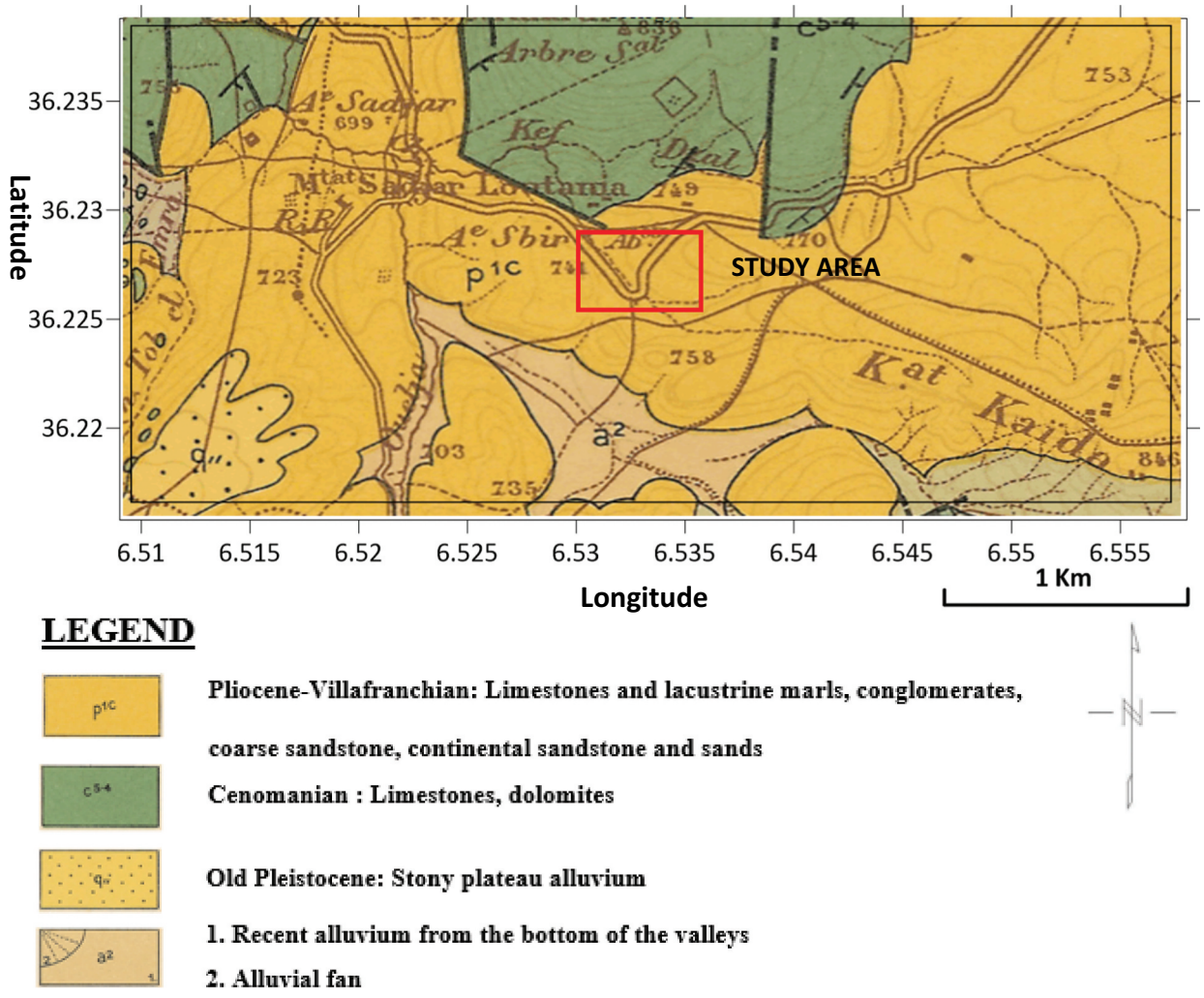

Figure 2. Geological map of the studied area (extracted from the geology of El Athmania, Scale 1/50.000) (Referenced sheet N°: 96B6–C26).

which joins further north to the Mediterranean (Mebarki 1982). In this context, Oued Kebir-Rhumel, drains several geological and hydrogeological areas. This heterogeneity of the basin causes different influences on the regime of the watercourses together with that due to the distribution of precipitation. The Neogene basin of Constantine Mila is a Miocene-Pliocene basin dominated by clay except for some outcrops of lacustrine limestone containing locally exploited resources. In addition, many horsts of neritic limestones emerge giving rise to hydrothermal karstic aquifers (Mebarki and Thomas 1988).

4. Material and methods

A systematic strategy has been undertaken in this study to evaluate the landslide's surface and subsurface properties. The electrical resistivity is a geophysical method that allows the investigation of the underground resistivity distribution. The method is based on injecting an electrical current of known intensity (I) into the subsurface (Figure 3) through one pair of electrodes (C_1 and C_2), those being inserted into the ground, and to measure the potential difference (ΔV) induced across another pair of electrodes (P_1 and P_2). Several factors affect the determined of resistivity such as the salinity, the porosity, the temperature, the water content and the mineralogical composition (Cebulski et al. 2020). The 2D resistivity technique has been described extensively by Telford et al. (1990) and Reynolds (2011). Various available electrode arrays are being used for subsurface resistivity studies. Most surveys are carried out using conventional arrays such as the Wenner, Schlumberger, dipole–dipole and pole–pole arrays (Loke et al. 2004). Each array has its advantages and disadvantages (Bayrak and Şenel 2012). Wenner array has been preferred in noisy site surveys owing to its quality detected signal (Cubbage et al. 2017). According to Drahor et al. (2006), the use of Wenner electrode array in landslide investigations produces similar reliable subsurface images as other sophisticated electrode arrays. So, it is not surprising that many case studies have been carried out using Wenner electrode array for landslides investigations (Khalil et al. 2018; Pappalardo et al. 2018; Falae et al. 2019; Hojat et al. 2019; Sutrisno et al. 2020; Tunçel et al. 2021).

5. 2D tomography acquisition

In order to obtain a 2D electrical resistivity image of the subsurface, it is necessary that the measurements be in 2D and uniform. For instance, the Wenner electrode array with 20 electrodes, shown in Figure 3, in which the distance between two electrodes is noted **a**, the first recorded measurement is done with the electrodes 1, 2, 3 and 4. The electrodes 1 and 4 are used for current injection and electrodes 2 and 3 to measuring the potential. The measurement point is plumb with the centre of this array. The whole array will then be moved by a distance **a** (Loke et al. 2004; Marescot LJCgatUo F. 2009; Nouioua et al. 2015). Electrodes 2 and 5 are then used for current injection and electrodes 3 and 4 for the potential measurement. The operation is repeated on the whole line of electrodes until the electrodes 18, 19 and 20. The apparent resistivity calculation is automatically done at the switch box of the resistivity metre. As a result, for the first acquisition level, there are 17 cases, i.e. (20–3 × **a**), due to the fact in the Wenner array characteristics is to keep a constant distance between all its electrodes. The next data acquisition level, an inter-

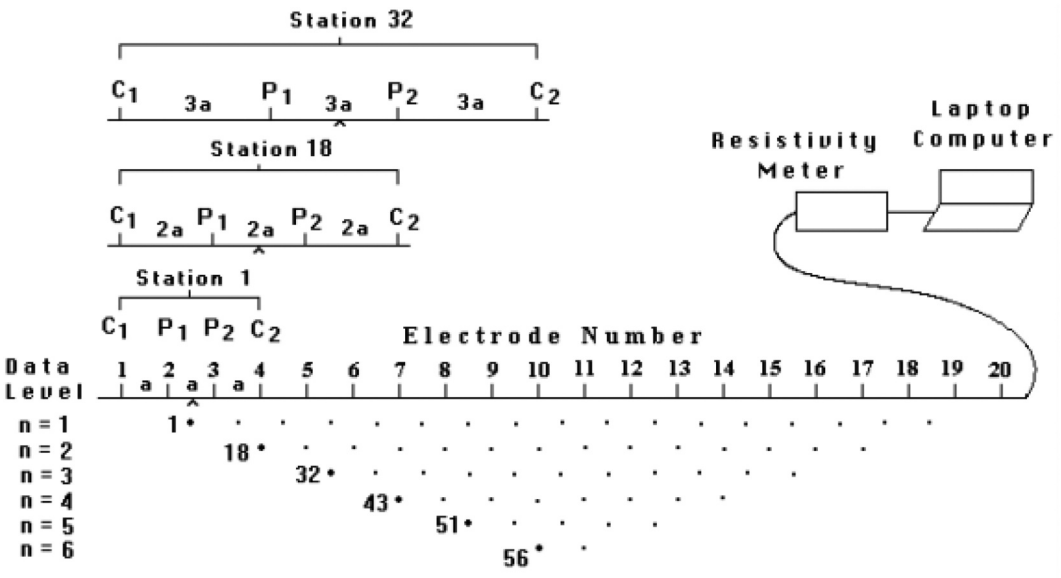

Figure 3. Measurements' sequence of a build-up pseudo-section of Wenner array (Nouioua et al. 2015).

electrode spacing equal to 2 × **a** is undertaken. The first measurement of the 2nd level will therefore involve the electrodes 1 and 7 for the injection of current and 3 and 5 for the measurement of the potential. The operation is repeated again up to the electrode 20. At this data level, there are 14 cases. For the 3rd level of acquisition there are 11 possibilities. The depth of investigation is set by varying the distance between the electrodes (Marescot LJCgatUo F. 2009). The measurements of every acquisition level are made with 4 × **a**, 5 × **a**, etc. (There are six data levels for the 20 electrodes of the Wenner array.)

In this study, the Wenner array has been applied due to its strong signal strength, this electrode array is applied for five profiles along and across the landslide. Three electrical profiles were executed perpendicular to the sliding path of 115 m length of each at slightly different elevation and two other profiles with a length of 69 m, along the slip direction (Figure 4), with an inter-electrode spacing of 5 and 3 m, respectively. The first profile (P_1) is located in the toe portion of the landslide and both profiles two and three (P_2 and P_3) were undertaken at the crest portion of the landslide body. The profile four (P_4) is located along the slope on the left flank, while the profile five (P_5) is located along the slope on the right flank slip (Figure 4). The measurement's sequence in collecting the 2D apparent resistivity data was carried out using a Syscal Junior Switch-48 electrodes resistivity metre (IRIS, France). The first three profiles (P_1, P_2 and P_3) were oriented NNW/SSE, while the others (P_4 and P_5) were oriented WSW/ENE, as shown in Figure 4.

Detailed informations regarding the positions of the conducted ERT profiles of Figure 4 are listed in Table 1. The borehole investigation data in combination with resistivity inverted sections were analysed,

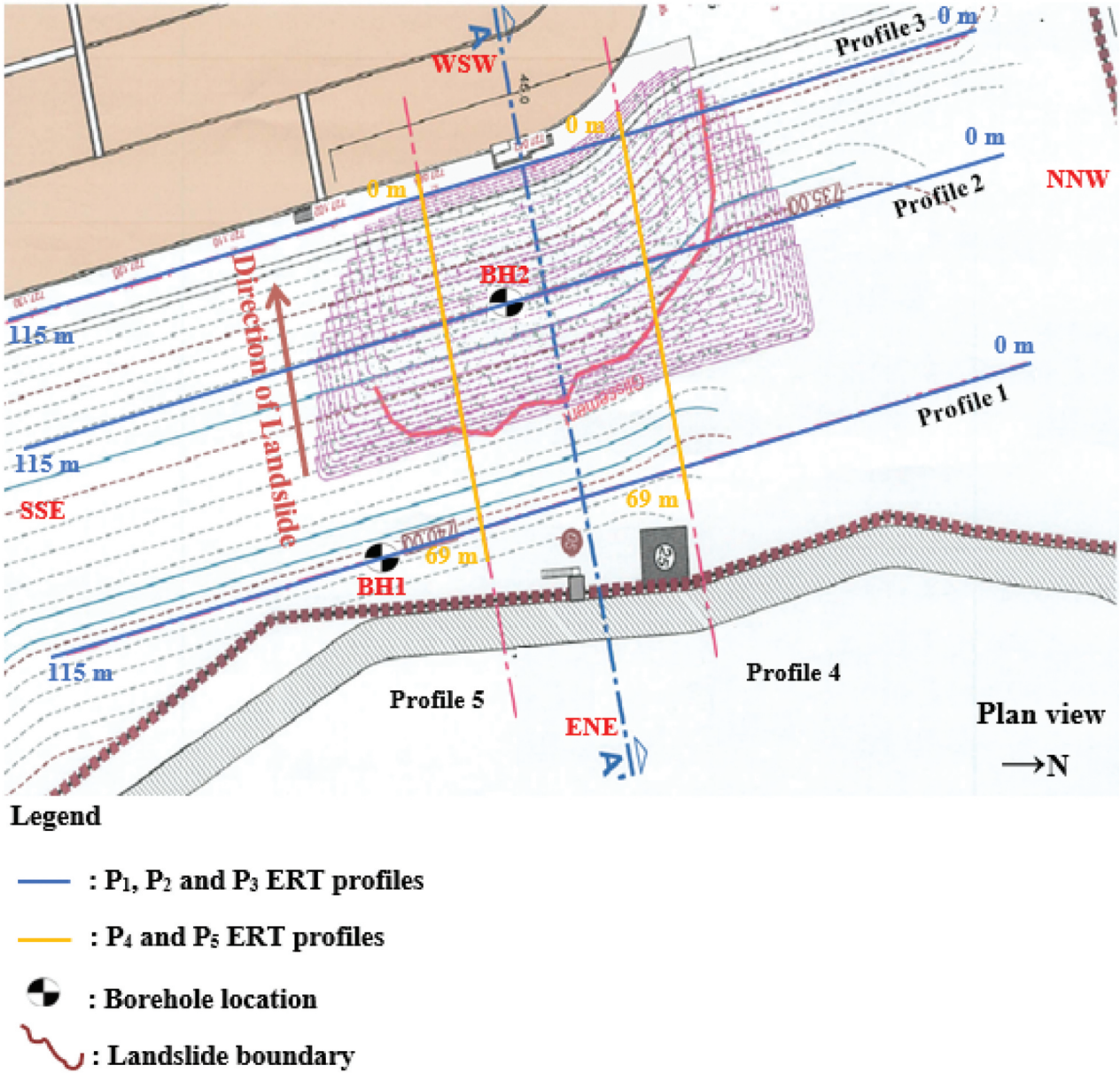

Figure 4. Topographic map of the landslide showing, the layout plan of electrical resistivity profiles and the locations of boreholes.

Table 1. Geographical coordinates of ERT survey profiles.

ERT profiles N°.	Coordinates of the conducted ERT profiles			
	Profile starting coordinates		Profile ending coordinates	
	Latitude	Longitude	Latitude	Longitude
P_1	36°13′38.54″N	6°31′54.18″E	36°13′35.02″N	6°31′55.86″E
P_2	36°13′38.61″N	6°31′52.65″E	36°13′34.96″N	6°31′54.32″E
P_3	36°13′38.13″N	6°31′51.52″E	36°13′34.52″N	6°31′53.41″E
P_4	36°13′36.59″N	6°31′52.27″E	36°13′37.18″N	6°31′55.04″E
P_5	36°13′35.94″N	6°31′52.57″E	36°13′36.58″N	6°31′55.24″E

Table 2. Parameters of the electrical resistivity tomography (ERT) field survey.

ERT profiles N°.	Resistivity metre system	Electrode Array	Number of electrodes	Inter-electrode spacing (m)	Total profile length (m)
P_1	Syscal Junior	Wenner	24	5	115
P_2	Syscal Junior	Wenner	24	5	115
P_3	Syscal Junior	Wenner	24	5	115
P_4	Syscal Junior	Wenner	24	3	69
P_5	Syscal Junior	Wenner	24	3	69

on one hand to check on the landslide features in terms of lithology and material and on the other hand, to define the probable surface of rupture and to estimate the thickness of the sliding layer, as carried out in other reported studies (Bellanova et al. 2016; Kristyanto et al. 2017, 2018; Rezaei et al. 2019). The parameters of ERT field measurements are described in Table 2.

6. Results and discussion

The raw apparent resistivity data were processed using the *Res2Dinv* program. This program is based on least-squares inversion of apparent resistivity pseudo-sections using a quasi-Newton method (Loke and Barker 1996). The program generates an inverted resistivity-depth section for the profile line based on the robust constrained L_1-norm (blocky) least-squares method (deGroot-Hedlin and Constable 1990; Loke et al. 2003). *Res2Dinv* uses the finite difference (FD) and finite element methods (FEM) to calculate the models of 2D forward response. The investigation depth increases with the increasing distance inter-electrodes. The maximum investigated depths of such array for the perpendicular and parallel profiles are around 20 m and about 12 m, respectively.

A first look at the inverted resistivity sections of all electrical profiles, it can be noticed that the resistivity varies within a moderate range; i.e. a minimum of 2 Ωm to a maximum of 70 Ωm and goes to even higher. Meanwhile, the root-mean-square error (RMSE) ranges from 1.77% to 9.4% which is estimated between measured and calculated apparent resistivities. For all ERT profiles the range of the electrical resistivity values is limited. According to the inverted images of resistivity (Figure 5a-e), there are two dominant facies. The first one is marked by low resistivity signature values ranging from 1.38 to 6.20 Ωm; this corresponds to wet clays (by water presence) which could be the reason of observed degradations in the studied site. This formation shows that there are layers likely to be at the origin of the landslide at a depth of 10.5 m and at extent depths from 17.5 and 20 m. Other facies present resistivity values ranging from 6.20 to 19 Ωm. These are moderately humid and more or less tuffaceous clays. The formations of medium to high resistivity values (19 to 70 Ωm).

Figure 5a the inverted section of the first profile (P_1), which is composed of a conductive layer situated between more or less resistant zones indicated by blue-light blue colours characteristic of a low resistivity signature with values (less than 4 Ωm). This is interpreted as the red clay material. The interface between the conductive zone and the underlying layers constitutes the slip line. This is clearly visible, moderately at a depth of around 10.5 m. The Figure 5(b) shows the cross-section of the inverted image of the profile P_2. This ERT image configures the sliding zone. The low resistivity area is directly under the sliding head, this explains the mass that occurred in this area. If we consider the difference in side between this profile and the first one, it can be deduced that the upper and the lower limits of the conductive clay layer constitute two levels of sliding (at depths of 10.5 m and between 17.5 and 20 m). It can be observed, that this zone of clay having a low resistivity constitutes the displaced body of the landslide. Despite the difference in altitude, if we compare in depth the profile P_3 (Figure 5c) and both profiles of P_1 and P_2, we note that the layer of a relatively low resistivity always exists and that it could generate unstable layers in the case of an increase in the water content (by infiltrations of rainwater or rising groundwater level (GWT)). Such a formation presents the continuity of low resistivity facies in the investigated area, already revealed by the two first profiles. Figure 6(a-d), reveals the landslide movement on the crest slope that is created by surface rupture, displaced materials and main scraps on the left and right flanks, respectively. Figure 5(d), shows the inverted section of the profile P_5 (without

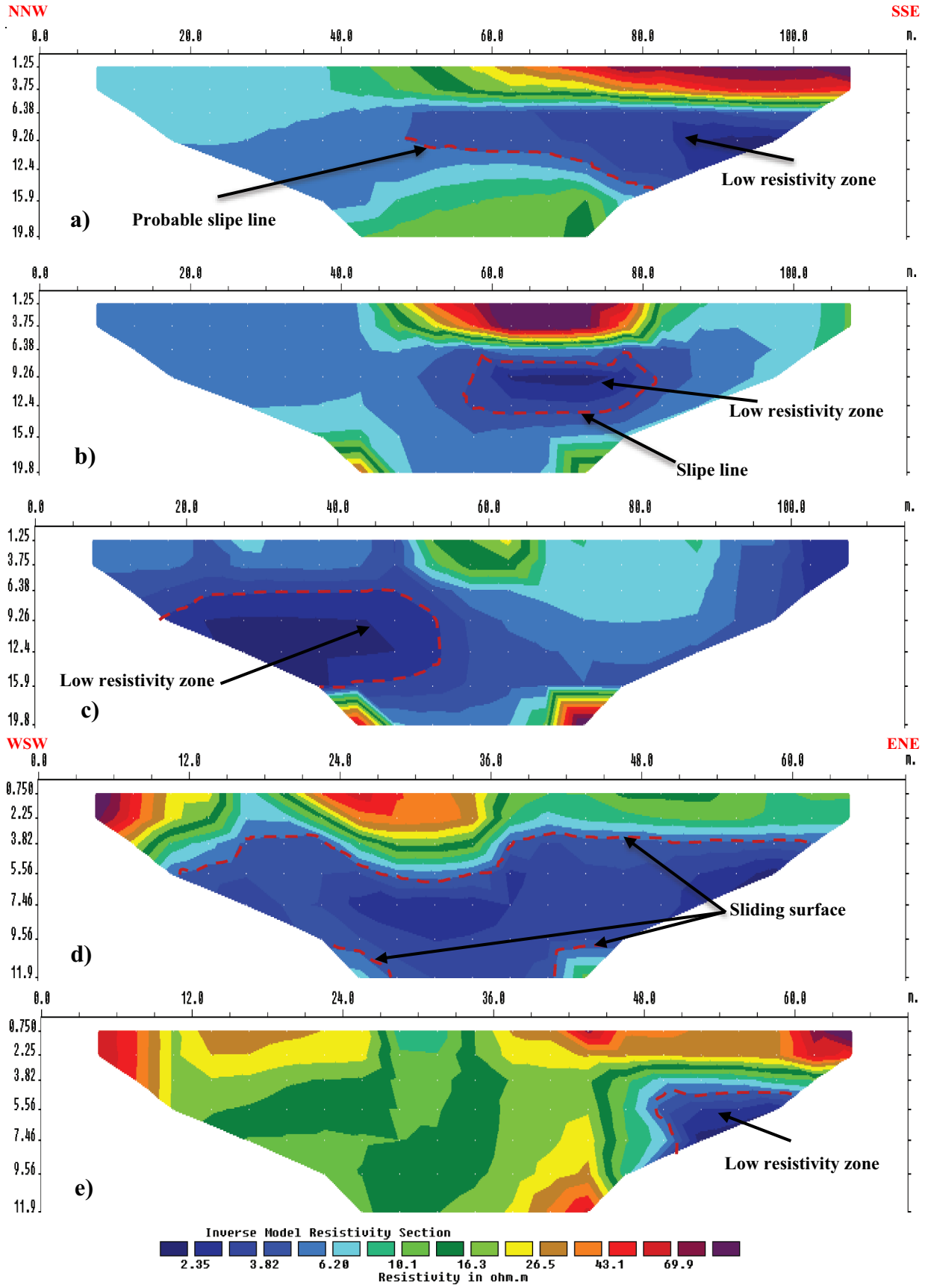

Figure 5. Inverted 2D resistivity sections of all electrical resistivity profiles: (a) profile 1, (b) profile 2, (c) profile 3, (d) profile 4 and (e) profile 5.

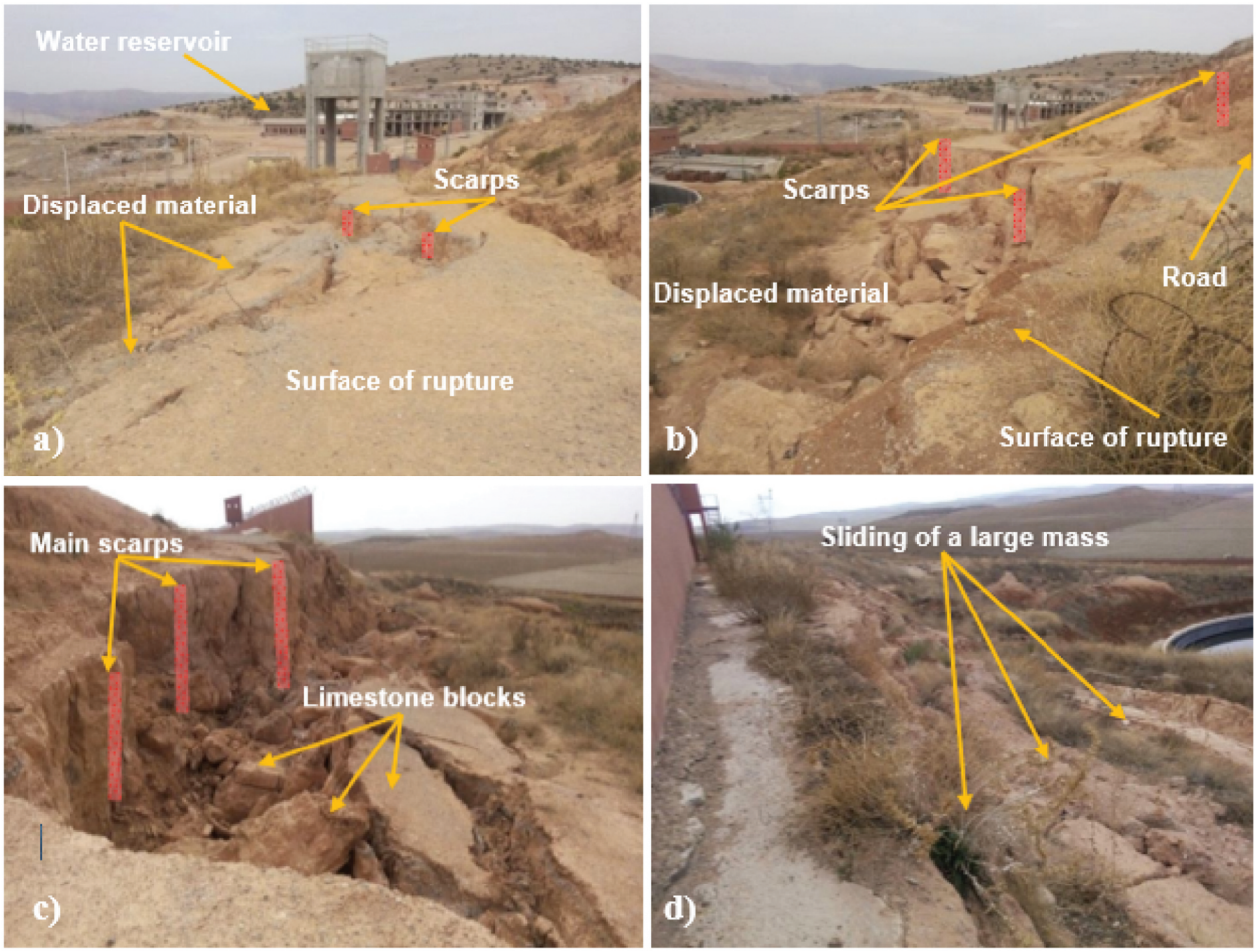

Figure 6. Landslide movement indications on the crest slope were manifested by scarps and displaced materials: (a, b) overview of the left flank; c and d) overview of the right flank.

topography correction). The ERT image is divided into two zones. The moderate resistivity values ranging from 7 Ωm to 30 Ωm, were recorded in the zone close to the top surface at a depth of about 0–4 m, and the zone with a lower resistivity, which comes just underneath the top zone indicated by the dark-blue colour, of a value that is less than 3 Ωm, is interpreted as red clay material.

These interpretations' results are in accordance with the lithological data from the first borehole of BH1 (its position is indicated in Figure 4). The image clearly illustrates how the sliding surface is affecting the studied area. By following the slip direction, over a length of about 60 m and at a depth of 12 m, it is seen that the conductive zone is predominant in this profile. It presents two surfaces of rupture, an upper surface responsible for the disorders observed along the slide and a lower surface which would be at the origin of the main movement. The sliding surface is deduced from the boundaries between the near surface layer, which has a relatively high resistivity mobilised material and the conductive clays. Figure 5(e), shows the inverted section of the profile P_5. Herein, it is likely that the zone could generate movements is only at the toe of the slope, and indication that the sliding zone is well limited (presence of an unstable zone). Based on the obtained results of the inverted images of the ERT lines of P_2 and P_4, it is possible to calculate approximately the volume of the displaced material; bearing in mind the following considerations: the surface of rupture at a depth of 10 m and a width of the slip zone where the conductive layer 35 m to 40 m (P_2) and the continuity of the latter according to the slip direction estimated by 50 m. Figure 6(a, b) shows an overview on the crest of the slope, the detachment and collapse of an important part of the slope have revealed the presence of ruptures and the opening of very void cracks that cut deep into the slope. Landslide of important mass revealing appear of the morphology in tiers, which is presented in Figure 6(c, d). The latter illustrates the surface of rupture and the metric escarpments at the top of the slope. Several vertical visible cracks are also observed throughout the right part of the landslide area. The landslide causes a significant collapse of the surface formations and the cracks at the top of the slope are very open and deep (Figure 6(c, d)). The presence of water and the geological formations sensitive to the presence of water has probably contributed to the starting of the landslide, whose volume can be roughly estimated by about 20.000

m^3. Groundwater presence is one of the major factors for triggering landsliding, soil instability and their occurrence. However, landslide presence decreases the factors of safety of slopes, especially, in soils of highly saturated state. Therefore, the seismic solicitations and activities play potential sources in the instability of the area and generating the landslides. In our study, the seismic activities have not contributed to the area instability.

7. Geotechnical reconnaissance of the site

In order to define the subsoil properties and its lithology constitution of the studied zone, as well as to know the layer of soil likely to slip. Therefore, it appears necessary to conduct a calibration borehole in this area. In this context, two boreholes (named here BH1 and BH2) were carried out in the studied zone. The total depth of the first borehole (BH1) was 20 m. The location of borehole was proposed based on the alignment of the first ERT profile (P_1) as depicted in Figure 4. The BH1 is equipped with inclinometer tube, while the total depth of the second borehole (BH2) was 15 m. The BH2 is located at the middle part of the second ERT profile (P_2) (Figure 4). In this study, the geotechnical investigations aim to characterise the subsoil. In the lithology of the studied zone, two main shallow subsurface layers have been basically encountered for both boreholes. The first one of the BH1 is constituted of a brown to beige tuffaceous clay more or less consolidated, with the presence of alveolar limestone blocks from the ground surface to 2.5 m of depth. The second one is composed by slightly tuffaceous red clay slightly humid and compact ranging from 2.5 to 20 m of depth. In addition, the BH2 lithology, consists from the top soil to a depth of 1.8 m, a tuffaceous clay with the presence of alveolar limestone blocks and from 1.8 m to 15 m, is made of a red clay lightly tuffaceous, slightly humid and compact. The inclinometer measurements method consists of inserting an inclinometric probe into a tube provided with four guide grooves and measuring at different depths in 50 cm units. For each measurement step, the probe's accuracy is between 0.01 and 0.1 mm. The angle that the axis of the guide tube element makes with the vertical. The orientation of the tube in the presumed direction of sliding is represented by the direction (−A/A+) always referring to geographic north. The inclination of the guide tube, with respect to the vertical, is obtained by moving the probe with a constant step equal to the length of the probe (50 cm) and repeating the same procedure at different time intervals. The inclinometric measurement carried out at the level of the BH1 cored borehole and after examination of the resulting graph presented below (see Figure 7), representing the displacement in the direction −A and A+, made it possible to locally detect the variations in inclination of the tube and to know the possible position of displacements. The direction to the first reading 001 presents a significant (minimum) value at 13 m depth, with a displacement of 2 mm to 3 mm. The second reading 002 (30 days after reading 001): presents also a significant (minimum) value at 10 m depth, with a displacement of 2 mm and another

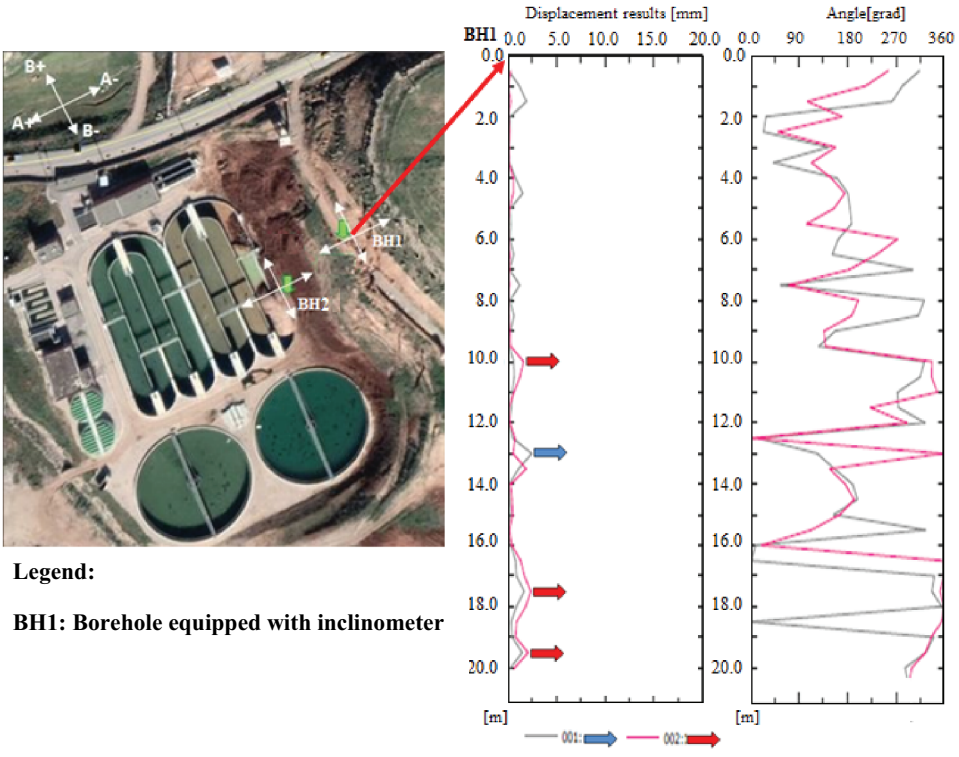

Legend:

BH1: Borehole equipped with inclinometer

Figure 7. Inclinomeic measurements installed in the borehole BH1.

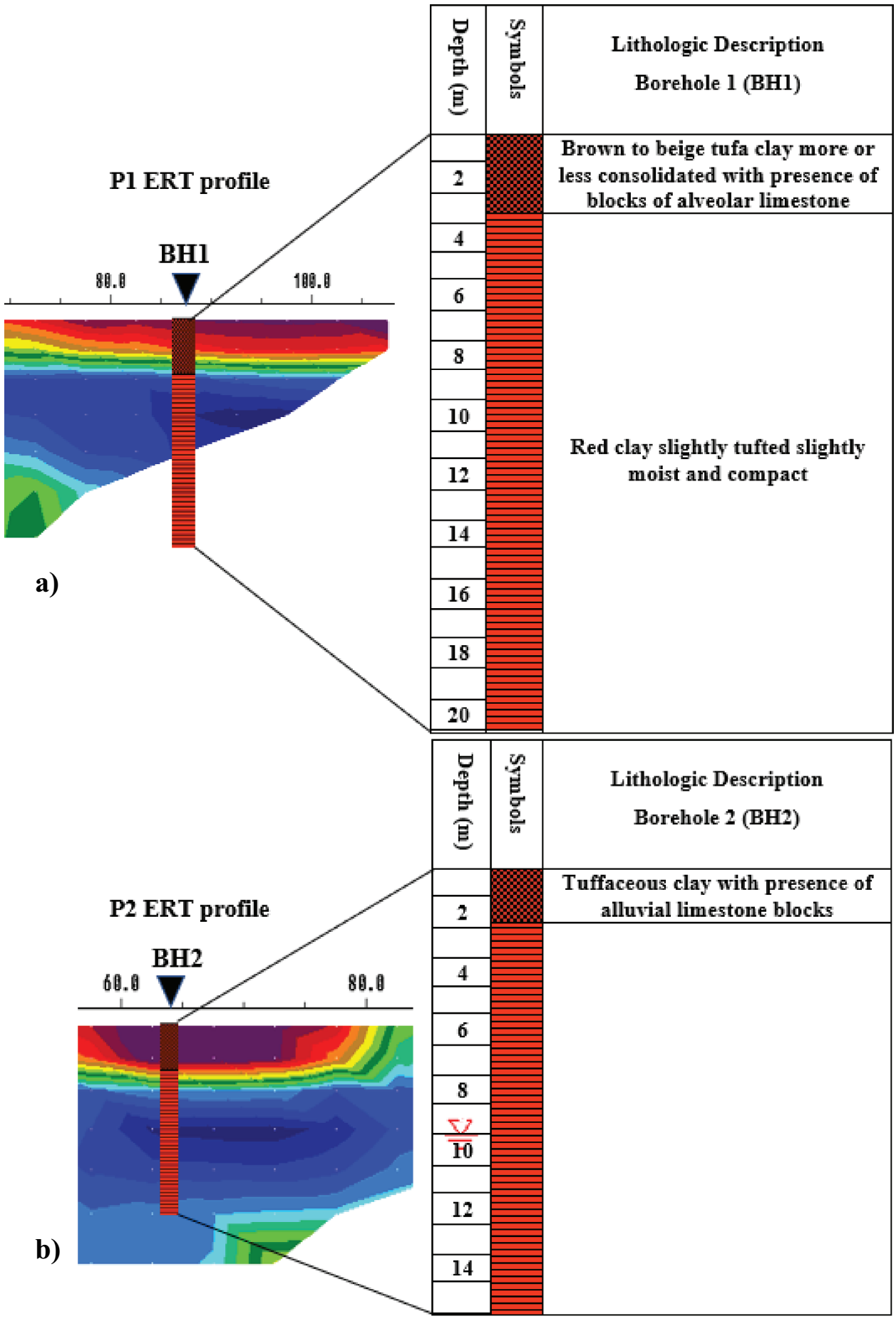

Figure 8. Correlation between 2D inverted resistivity sections of ERT profiles and the survey site lithology, deduced from well: (a) P_1 ERT with BH1 and (b) P_2 ERT with BH2.

value between 17.5 and 19.5 m depth of about 2.5 mm. The direction to B did not present a significant value. This arrangement is in perfect agreement with the local geology and the analysis of the inclinometric measurements led to suspect a sliding surface at 10 m, 13 m and between 17.5 and 19.5 m in depth and at displacements of the order of 2 to 3 mm.

The 2D electrical resistivity tomography result for the first profile (P_1), which intersects the borehole BH1 at around 86 m distance from the starting point of the first profile as shown in Figure 8a. Moreover, the 2D ERT result for the second profile (P_2), which intersects the borehole BH2 at around 65 m distance from the first electrode, is depicted in Figure 8b. It is noted, that the ERT pseudo-sections show the presence of low resistivity ranging from less than 2 up to 6 Ωm, at interval depth from 6 up to 16 m, as indicated in Figure 8(a,b). The results of ERT images of profiles P_1 and P_2 with the lithology of the borehole data of BH1 and BH2 show a good correlation. Thus, the inclinometric measurements analysis allowed to suspect that the slip surface at 10 m, 13 m and between 17,5 m and 19,5 m of depth and the displacements were of the order of 2 mm to 3 mm. It can be summarised that the ERT (ERT) method shows a good agreement with both of the borehole informations and the inclinometer measurements (Figure 8).

8. Conclusion

In summary, an integrated approach applied to characterise the internal structure of the landslide from geophysical data is presented in this paper. The use of geophysical tool of ERT (ERT) method is well suited for investigating and characterising the internal structure of Ali Mendjeli landslide. The obtained results from the recorded electrical resistivities along fives profiles using Wenner electrode array were carried out in the landslide zone reveal a structure composed of two formations of very distinct resistivities. The first formation is of low resistivity, and of a high moisture content due to rainwater infiltration or the rise of the groundwater table (GWT) level. A second formation represented by moderately water content clays more or less tuffaceous, presenting moderate resistivity values compared to the first formation. The results of ERT images show the sliding surfaces at different depths characterised by low resistivity values and linked to the saturation state of the landslide zone. The sliding surfaces constitute the interface between the two formations encountered. The analysis of the inverted 2D ERT images, and particularly the profiles P_3 and P_4, allowed to deduce that the failure surface generating the landslide is located at the crest of the slope given the presence of a conductive layer at depth in profile P_3 and its continuity along the landslide in profile P_4. Based on the obtained results, the volume of the mass of earth in movement can be calculated in an approximate way. If we consider a sliding surface at a depth of 10 m, a width of the slide zone or the span of the conductive layer which is 35 m to 40 m and the continuity of the latter along the slide direction which is estimated at 50 m. The landslide volume is roughly estimated to about 20.000 m^3. The combined ERT images, geotechnical investigations (inclinometric tests) and field observations have revealed the sliding surfaces and define/estimate the displaced material mass. This study illustrates underlines the potential of the ERT method as detecting tool in landslide inspections. Therefore, ERT is a powerful tool for delineating the boundaries of landslide.

Acknowledgements

The authors would like to express their thanks and gratitude to the company of "Laboratoire des Travaux Publics de l'Est (LTPE) for permitting the use and publication of the resistivity data and their help to complete this study. The first author also thanks the STEP Project Director Mr. Boucherite Mohamed Chaouki, from Laboratoire National de l'Habitat et de la Construction (LNHC). The authors are grateful to Pr. Boubaya Djamel (Larbi Tebessi University, Tebessa) for providing us with the geological map of the area of interest.

Disclosure statement

No potential conflict of interest was reported by the author (s).

ORCID

Kamel Hebbache http://orcid.org/0000-0002-4409-3689

References

Akpan AE, Ilori AO, Essien NU. 2015. Geophysical investigation of obot ekpo landslide site, Cross River state, Nigeria. J African Earth Sci. 109:154–167. doi:10.1016/j.jafrearsci.2015.05.015.

Bayrak M, Şenel L. 2012. Two-dimensional resistivity imaging in the Kestelek boron area by VLF and DC resistivity methods. J Appl Geophys. 82:1–10. doi:10.1016/j.jappgeo.2012.03.010.

Bellanova J, Calamita G, Giocoli A, Luongo R, Macchiato M, Perrone A, Uhlemann S, Piscitelli SJEG. 2018. Electrical resistivity imaging for the characterization of the Montaguto landslide (southern Italy), Engineering Geology. 243:272–281. doi:10.1177/1535370217745302.

Bellanova J, Calamita G, Giocoli A, Luongo R, Perrone A, Lapenna V, Piscitelli S. 2016. Electrical Resistivity Tomography surveys for the geoelectric characterization of the Montaguto landslide (southern Italy). Nhess 28 . Discussions.1–17.

Bogoslovsky V, Ogilvy A. 1977. Geophysical methods for the investigation of landslides. Geophysics. 42(3):562–571. doi:10.1190/1.1440727.

Casagli N, Tofani V, Sassa K, Bobrowsky PT, Takara K. 2020. Understanding and Reducing Landslide Disaster Risk: volume 3 Monitoring and Early Warning. Berlin, Germany: Springer Nature.

Cebulski J, Pasierb B, Wieczorek D, Zieliński AJC. 2020. Reconstruction of landslide movements using digital elevation model and electrical resistivity tomography analysis in the Polish Outer Carpathians, CATENA. 195. 104758.

Coiffait P-E. 1992. Un bassin post-nappes dans son cadre structural: l'exemple du bassin de Constantine . Algérie nord-orientale. Nancy 1, Doctorate thesis, Nancy I université (405 p).

Crawford MM, Zhu J, Webb SE. 2015. Geologic, geotechnical, and geophysical investigation of a shallow landslide, eastern Kentucky. Environ Eng Geosci. 21(3):181–195. doi:10.2113/gseegeosci.21.3.181.

Cubbage B, Noonan GE, Rucker DFJP, Geophysics A. 2017. A modified Wenner array for efficient use of eight-channel resistivity meters, Pure and Applied Geophysics. 174 (7):2705–2718.

deGroot-Hedlin C, Constable S. 1990. Occam's inversion to generate smooth, two-dimensional models from magnetotelluric data. Geophysics. 55(12):1613–1624. doi:10.1190/1.1442813.

Drahor MG, Göktürkler G, Berge MA, Kurtulmuş TÖJEG. 2006. Application of electrical resistivity tomography technique for investigation of landslides: a case from Turkey, Environmental Geology. 50(2):147–155.

Falae PO, Kanungo DP, Chauhan PKS, Dash RK. 2019. Electrical resistivity tomography (ERT) based subsurface characterisation of Pakhi Landslide, Garhwal Himalayas, India. Environ Earth Sci. 78(14):1–18. doi:10.1007/s12665-019-8430-x.

Giano SI, Lapenna V, Piscitelli S, Schiattarella M. 2000. Electrical imaging and self-potential survayes to study the geological setting of the Quaternary, slope depositsin the Agri high valley. (Southern Italy): Annals of Geophysics.

Hebbache K, Boubaya D. 2022. 2D electrical resistivity tomography (ERT) and GPR methods for soil characterization near Tiaret, northwest of Algeria—a case study, Arabian Journal of Geosciences. 15(22):1–12.

Hojat A, Arosio D, Ivanov VI, Longoni L, Papini M, Scaioni M, Tresoldi G, Zanzi L. 2019. Geoelectrical characterization and monitoring of slopes on a rainfall-triggered landslide simulator, Journal of Applied Geophysics. 170. 103844.

Ismail NI, Yaacob WZW. 2018. Application of electrical resistivity tomography (ERT) for slope failure investigation: a case study from Kuala Lumpur. Jurnal Teknologi. 80(5). doi:10.11113/jt.v80.11624.

Khalil MA, Bobst A, Mosolf JJP, Geophysics A. 2018. Utilizing 2D electrical resistivity tomography and very low frequency electromagnetics to investigate the hydrogeology of natural cold springs near Virginia City. Southwest Montana. 175(10):3525–3538.

Kherrouba H, Lamara M, Contribution of electrical tomography to the study of landslides in Texenna Region (Northeast Algeria). Conference of the Arabian Journal of Geosciences, Hammamet, Tunisia; 2018: Springer.

Kristyanto TH, Indra TL, Syahputra, R, Tempessy, AS. 2017. Determination of the landslide slip surface using electrical resistivity tomography (ERT) technique. In: Workshop on World Landslide Forum. Berlin, Germany: Springer, 53–60.

Lee -C-C, Yang C-H, Liu H-C, Wen K-L, Wang Z-B, Chen Y-J. 2008. A Study of the hydrogeological environment of the lishan landslide area using resistivity image profiling and borehole data. Eng Geol. 98(3–4):115–125. doi:10.1016/j.enggeo.2008.01.012.

Loke MH, Acworth I, Dahlin T. 2003. A comparison of smooth and blocky inversion methods in 2D electrical imaging surveys. Explor Geophys. 34(3):182–187. doi:10.1071/EG03182.

Loke MH, Barker RD. 1996. Rapid least□squares inversion of apparent resistivity pseudosections by a quasi□Newton method1. Geophysical Prospecting. 44(1):131–152. doi:10.1111/j.1365-2478.1996.tb00142.x.

Loke MH, Loke MH, Ogilvy RD, Meldrum PI. 2004. Tutorial: 2-D and 3-D electrical imaging surveys. Journal of Contaminant Hydrology. 68(1–2):1–22. doi:10.1016/S0169-7722(03)00142-6.

Marescot LJC 2009. Electrical surveying: part 2.

Margottini C, Canuti P, Sassa K. 2013. Landslide Science and Practice: volume 2: early Warning. In: Instrumentation and Monitoring. Springer Science & Business Media. doi:10.1007/978-3-642-31445-2

Mebarki A . 1982. Le Bassin du Kébir-Rhumel (Algérie): hydrologie de surface et aménagement des ressources en eau. éditeur inconnu (Université de Nancy II (France). p 304).

Mebarki A, Thomas C, ORSTOM, Paris. 1988. Analyse des relations entre écoulements superficiels et souterrains à partir des hydrogrammes des cours d'eau. Application Au Bassin du Kébir-Rhumel Dans le Constantinois (Algérie). 3(2):89–103.

Hebbache K, Mellas M, Boubaya D. 2016. APPLICATION OF 2D SURFACE ELECTRICAL RESISTIVITY TOMOGRAPHY TO DETECT THE UNDERGROUND CAVITIES A CASE SITE STUDY: TOLGA AREA. (ALGERIA): Courrier du Savoir.

Nordiana M, Azwin I, Nawawi M, Khalil A. Geophysics. 2018. Slope failures evaluation and landslides investigation using 2-D resistivity method, NRIAG Journal of Astronomy and Geophysics. 7(1). 84–89.

Nouioua I, Fehdi C, Boubaya D, Serhane B, Djellali A. 2015. Mapping underground cracks using 2D electrical resistivity tomography: the case of the landslide of Kef Essenoun phosphate deposit, Djebel Onk (northeast of Algeria). Arab J Geosci. 8(10):7731–7738. doi:10.1007/s12517-014-1769-0.

Osinowo OO, Falufosi M. Geophysics. 2018. 3D Electrical Resistivity Imaging (ERI) for subsurface evaluation in pre-engineering construction site investigation NRIAG Journal of Astronomy and Geophysics. 7(2). 309–317.

Pappalardo G, Imposa S, Barbano M, Grassi S, Mineo SJL. 2018. Study of landslides at the archaeological site of Abakainon necropolis (NE Sicily) by geomorphological and geophysical investigations, Landslides. 15(7):1279–1297.

Reci H, Muceku Y, Jata I. 2013. The use of ERT for investigation of berzhita landslide, Tirana area, Albania. Landslide Science and Practice. Berlin/Heidelberg, Germany: Springer; p. 117–123.

Reynolds JM. 2011. An introduction to applied and environmental geophysics. Oxford: Wiley: John Wiley & Sons.

Rezaei S, Shooshpasha I, Rezaei H. 2018. Empirical Correlation between Geotechnical and Geophysical Parameters in a Landslide Zone (Case Study: naigeschal Landslide). Earth Sci Res J. 22(3):195–204. doi:10.15446/esrj.v22n3.69491.

Rezaei S, Shooshpasha I, Rezaei H, Environment t. 2019. Reconstruction of landslide model from ERT, geotechnical, and field data. Nargeschal Landslide, Iran. 78(5):3223–3237.

Samodra G, Ramadhan MF, Sartohadi J, Setiawan MA, Christanto N, Sukmawijaya A. 2020. Characterization of displacement and internal structure of landslides from multitemporal UAV and ERT imaging. Landslides. 17 (10):2455–2468. doi:10.1007/s10346-020-01428-0.

Sutrisno, Wardani, IK , Heriyanto, Suaidi, DA. The Wenner configuration of geoelectrical method to identify landslide areas on protocol street (case study: jl. Kambal–Mulyorejo R, Ngantang M. Eds. AIP Conference Proceedings Melville, USA; 2020: AIP Publishing LLC. doi:10.1063/5.0016330

Telford WM, Telford W, Geldart L, Sheriff RE. 1990. Applied geophysics. United Kingdom: Cambridge university press.

Tunçel A, Kıncal C, Berge Majajo G. 2021. Site investigation of a landslide site and its surroundings: a case study at Eğridere district, northern Izmir city. Turkey. 14(20):1–16.

Zhuang Y, Xing A. 2020. Electrical Resistivity Tomography (ERT) Based Investigation of Two Landslides in Guizhou, China Nicola, C, Veronica, T, Kyoji, S, Peter T, B, Kaoru, T. In: Workshop on World Landslide Forum. Springer, Cham: Springer, 109–116.